ELSEVIER

International Journal of Mass Spectrometry 203 (2000) 165–175

International Journal of Mass Spectrometry

Gas phase reactions of CF_3O^- and $CF_3O^-H_2O$ with nitric, formic, and acetic acid

C. Amelynck*, N. Schoon, E. Arijs

Belgian Institute for Space Aeronomy, Ringlaan 3, B-1180 Brussels, Belgium

Received 7 July 2000; accepted 13 August 2000

Abstract

The reactions of CF_3O^-, $CF_3O^-H_2O$ and CF_3O^-HF with HNO_3, HCOOH, and CH_3COOH have been studied at room temperature in a flowing afterglow instrument. Apart from the reaction of CF_3O^-HF with CH_3COOH, all reactions proceed at the collision rate. Bare CF_3O^- ions react with the three acids mainly by fluoride transfer. An unambiguous identification of the reaction mechanisms of $CF_3O^-H_2O$ and CF_3O^-HF with the three neutral reactants is difficult to assess. The possibility to perform in situ measurements of HNO_3, HCOOH, and CH_3COOH concentrations in the atmosphere by chemical ionization mass spectrometry (CIMS), using a CF_3O^- ion source will be discussed. (Int J Mass Spectrom 203 (2000) 165–175) © 2000 Elsevier Science B.V.

Keywords: Chemical ionization; Ion/molecule reactions; Stratospheric trace gases; Nitric acid; Carboxylic acids

1. Introduction

In recent years, CIMS (chemical ionization mass spectrometry), or various versions of it, have been used by several research groups to measure trace gas concentrations in the atmosphere. This technique is based on the formation of specific product ions from the ion/molecule reactions of trace gases with precursor ions produced by an ion source mounted at one extremity of a flow tube (or drift tube), which is coupled to a mass spectrometer at the other extremity and through which the sampled air is flown.

The measurement of the ratio of product to source ions allows the derivation of the trace gas concentration if the ion residence time in the flow tube and the rate constants of the ion/molecule reactions involved are known. The CIMS method, first introduced in atmospheric research by Arnold and coworkers for the detection of stratospheric nitric acid [1], has been reviewed through 1993 by Viggiano [2]. It has now been extended and adapted under different forms for measurement of several other trace gases such as HCl, HF, HCN, SO_2, OH, H_2SO_4, and CH_3CN [3–10]. Specific applications lie in those fields where fast time-response measurements are required [11] or local phenomena are investigated such as polar atmospheric research [12] and the study of aircraft emissions [13,14].

Recently, Huey investigated the ion/molecule reactions of several atmospheric trace gases with CF_3O^- ions and found out that this ion was a promising source ion for CIMS applications in atmospheric research because of the very specific product ions formed with different atmospheric minor constit-

*Corresponding author. E-mail: crist.amelynck@bira-iasb.oma.be

PII S1387-3806(00)00321-3

uents [15]. As a result, we have used this ion in our balloon-borne instrument for the measurement of HNO_3, $ClONO_2$, and HCl in the stratosphere [16].

It turned out, however, that the $CF_3O^-H_2O$ ion was formed by the reaction with stratospheric water vapor with the source ion CF_3O^- to a larger extent than expected. This caused an additional complication for the data analysis, which prompted us to undertake some additional laboratory measurements of gas phase reactions of the CF_3O^- and $CF_3O^-H_2O$ ion [17]. With the aim of better understanding our previous data on nitric acid obtained in the stratosphere and also in an effort to set up some new CIMS reaction schemes for the detection of other atmospheric trace gases, we studied the reactions of CF_3O^- and $CF_3O^-H_2O$ with HNO_3, HCOOH, and CH_3COOH. The latter three gases play an important role in atmospheric chemistry.

Nitric acid, which is formed through the association of OH to NO_2, is a sink for NO_x in the stratosphere as well as in the troposphere through its removal by rain out and dry deposition. In the stratosphere, it plays an important role in the ozone chemistry by taking away the NO_x species, which lead to catalytic ozone destruction, and through its inclusion in aerosols [18,19]. In the troposphere, nitric acid also significantly contributes to acid rain [20]. Nitric acid has been measured in the atmosphere by optical remote sensing [19,21–24], filter collection [25], and CIMS [1–3,11–14,16].

Formic acid (HCOOH) and acetic acid (CH_3COOH) are the most abundant carboxylic acids in the troposphere. They were found to be ubiquitous components of the gaseous and aqueous phase of the lower atmosphere and of aerosol particles. In the gas phase, observed mixing ratios range from 0.05 ppbv in nonpolluted atmospheres to 16 ppbv in urban regions [26]. Sources of formic and acetic acids comprise natural and anthropogenic emissions as well as chemical transformation of organic precursor gases [26]. As they hardly react with other constituents in the atmosphere, their major sink is dry and wet deposition. As a result, they are major contributors to precipitation acidity, especially in remote areas [27]. Various in situ measurement techniques for HCOOH and CH_3COOH based on vapor collection by filters, mist chambers, and denuders have been developed and intercompared [28]. In addition, formic acid has been detected by infrared absorption spectroscopy using its line parameters at 1105 cm^{-1} [29–33] and acetic acid at 1176 [32] and 1183.8 cm^{-1} [33]. The spectroscopic quantifications still suffer from considerable discrepancies with the chemical measurements, but new determinations of the spectral parameters [34] may improve this situation. The first measurement of formic and acetic acid based on mass spectrometry was performed by Chapman et al., using atmospheric pressure chemical ionization [35]. These authors gave no details of the ion/molecule reactions involved in their measurement technique, and concentrations were derived using an empirical calibration method. Huey and Lovejoy reported that formic acid rapidly clusters with SiF_5^- and proposed this ion as a precursor ion for CIMS measurements of formic acid [36]. A more systematic approach was done by Reiner et al. [37], who performed CIMS measurement of formic and acetic acid with an aircraft-borne triple quadrupole mass spectrometer based on ion/molecule reactions with CO_3^- core ions, which were studied by Viidanoja et al. [38].

In this article, we report measurements of ion/molecule reactions of nitric, formic, and acetic acid with CF_3O^- and $CF_3O^-H_2O$ and discuss the possibility of using these reactions for CIMS measurements in the atmosphere.

2. Experiment

The ion/molecule reactions were studied in a stainless steel flowing afterglow apparatus at room temperature. The apparatus has been described thoroughly in a previous paper [17] and will therefore be discussed only briefly here. A schematic representation of the instrument and the reactant gas introduction systems is shown in Fig. 1. The apparatus consists of a 6.5-cm inner-diameter flow tube connected to a differentially pumped quadrupole mass spectrometer. The flow tube is separated into a low-pressure and a high-pressure section by a plate con-

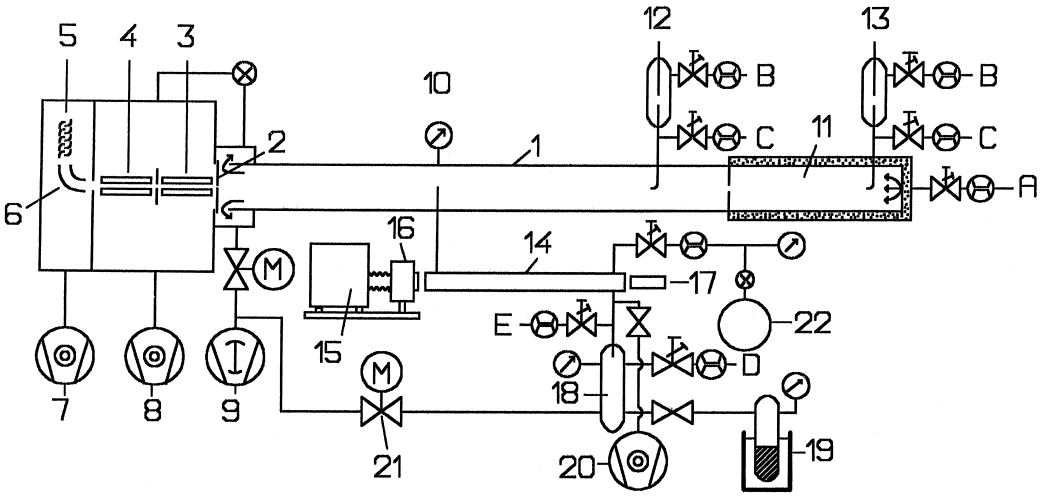

Fig. 1. Schematic representation of the laboratory apparatus. *A*, buffer gas inlet; *B*, Ar inlet; *C*, Ar+CF_3OOCF_3 inlet; *D*, E, Ar inlet; *1*, flow tube; *2*, polarisable inlet plate; *3*, octopole; *4*, quadrupole mass filter; *5*, secondary electron multiplier; *6*, deflecting lenses; *7*, *8*, turbomolecular pumps; *9*, rootspump; *10*, pressure sensor; *11*, flow tube high-pressure section (can be cooled with solid CO_2 pellets); *12*, discharge ion source; *13*, idem; *14*, optical absorption cell; *15*, deuterium lamp; *16*, monochromator; *17*, photomultiplier; *18*, HNO_3 dilution chamber; *19*, HNO_3 reservoir; *20*, turbomolecular pump; *21*, electronically controlled valve; *22*, 2-L glass bulb.

taining a hole 4 mm in diameter concentric with the axis of the flow tube. Reactant CF_3O^- ions were produced in a high-pressure ion source by adding small amounts of CF_3OOCF_3 to the afterglow of an Argon gas discharge. Pure helium (99.9999%) was used as the ion carrier gas at a flow rate of 75 STP (standard temperature and pressure; 0°C, 1 atm) cm^3 s^{-1}. On cooling the walls of the high-pressure part of the flow tube at −76°C, $CF_3O^-H_2O$ ions are formed in this section by a three-body reaction with residual water vapor impurities in the helium buffer gas (<0.5 ppmv as specified by the gas supplier). Apart from $CF_3O^-H_2O$, there is also formation of CF_3O^-HF and in some cases also $CF_3O^-F_2$ and $F^-CF_3OOF_3C$. By using very small concentrations of CF_3OOF_3C, the concentrations of these ions can be reduced, although not in a fully controllable way. Hydration of CF_3O^- was restricted to the cooled high-pressure region of the flow tube and did not take place in the low-pressure reaction zone, as was explained in a previous paper [17].

The reactant gases are introduced through a glass finger inlet at a distance of 43.4 cm from the mass spectrometer inlet. Nitric acid was purified by vacuum distillation of a liquid 3:2 HNO_3 (65% aqueous solution) : H_2SO_4 mixture. According to the triangular Gibbs diagram of the equilibrium composition of the liquid and vapor phase of the ternary $HNO_3/H_2SO_4/H_2O$ system, the HNO_3 mixing ratio of the vapor phase of this system should be better than 99% [39]. The pure nitric acid sample was stored in a glass reservoir at −60°C. During the measurements the reservoir was kept at 17.5°C. Pure HNO_3 leaving the reservoir through a capillary was diluted in Ar in a stainless steel dilution chamber, which has been described before [40]. A small part of the diluted Ar + HNO_3 flow leaves the dilution chamber through a second capillary and flows, together with an additional 0.17 STP cm^3 s^{-1} flow of Argon, through a 50-cm-long absorption cell (2.5-cm inner diameter) before entering the flow tube reactor. This cell is connected to the flow tube by a 10-cm-long × 0.2-cm internal diameter glass tube, which ends on the axis of the flow tube. The cell is fitted with Suprasil windows, and the HNO_3 concentration in it is obtained by optical absorption measurements at a wavelength of 186 nm where the absorption cross section is 1.580×10^{-17} cm^2 $molecule^{-1}$ [41]. The nitric acid con-

centration in the flow tube is derived by multiplying the concentration in the absorption cell with the ratio of the flow in the absorption cell to the total flow through the flow tube and with the ratio of the pressure in the flow tube to the pressure in the absorption cell [42].

Dilute $HCOOH/N_2$ and CH_3COOH/N_2 gas mixtures were prepared by transferring pure organic acid vapor (typically 1.3–4 mbar) from a twice-degassed liquid reservoir to an evacuated 2-L glass bulb. Then N_2 was added to a total pressure of about 1000 mbar. Liquid HCOOH and CH_3COOH were obtained from Aldrich and had a stated purity of, respectively, 97% and 99.7%.

Small flows (0.02–0.33 STP $cm^3\ s^{-1}$) of the dilute mixtures were added to the buffer gas flow using a commercial mass flow controller mounted between the gas reservoir (2-L glass bulb) and the absorption cell. In this case the latter is not used for optical measurements but merely serves to reduce the partial pressure of the carboxylic acids before they are introduced into the flow tube. It is well known that simple carboxylic acids such as HCOOH and CH_3COOH form dimers in the gas phase. This is taken into account in the calculations of the HCOOH and CH_3COOH concentrations in the reaction zone by calculating the flow of formic (or acetic) acid Q_{ca} through

$$Q_{ca} = \frac{p_m + 2p_d}{p_T} \times Q_m, \quad (1)$$

where p_m, p_d, and p_T are the partial pressure of monomers, partial pressure of dimers, and total pressure in the gas container, respectively, and Q_m is the total flow (nitrogen + carboxylic acid flow) as measured by the flow meter. The monomer/dimer equilibrium ratio in the glass bulb was calculated using the formulas of Büttner and Maurer [43]:

$$-\ln K_{fa} = -18.0763 + 7130.9/T \quad (2)$$

$$-\ln K_{aa} = -19.1001 + 7298.7/T \quad (3)$$

Where K_{fa} and K_{aa} are the monomer/dimer equilibrium constants for formic and acetic acid, respectively (in atm^{-1}), and T is the temperature (in K). In applying Eq. (1), it is assumed that all dimers exiting the reservoir are converted to monomers in the 50-cm absorption cell. This is a reasonable assumption as the pressure in the intermediate glass cell is >100 times smaller than the pressure in the 2-L reservoir. Furthermore, the average residence time of the gas in the glass cell is about 5 s, and the lifetime of the dimers is expected to be only a few milliseconds [44].

It was also shown by Finkbeiner et al. [45] that the corrected dilute mixture method (correction based on the equilibrium between monomers and dimers) as we applied it for producing controlled formic acid flows agreed satisfactory with a method based on the pyrolysis of *t*-butyl formate.

As organic acid vapors are known to be sticky compounds, several dilute mixtures with different carboxylic acid contents have been used to check if errors were made in quantifying carboxylic acid concentrations. Rate constants k for the ion/molecule reactions are calculated from the primary ion signals $[X^-]$ at different reactant gas concentrations in the flow tube by using the formula

$$-\ln\left(\left[\frac{X^-}{X_0^-}\right]\right) = k \times \tau \times [Y], \quad (4)$$

where $[Y]$ denotes the reactant gas concentration, $[X_o^-]$ is the primary ion signal without addition of reactant gas to the reaction zone, and τ is the reaction time. The latter was measured experimentally by pulsing an electrically insulated metal ring located close to the reactant gas inlet and by recording synchronously the arrival of the resulting disturbance in the ion flow at the detector by the use of a multichannel scaler.

3. Results

3.1. Reactions with nitric acid

The reaction of CF_3O^- with HNO_3 was studied at pressures ranging from 0.66 mbar to 1.33 mbar. A pressure-independent rate constant of $(2.3 \pm 0.2) \times 10^{-9}\ cm^3\ molecule^{-1}\ s^{-1}$ was obtained. As was already

reported by Huey et al. [15], two pathways for the reaction of CF_3O^- with HNO_3 were observed: a fluoride transfer channel (Eq. [5a]) and a proton transfer channel [Eq. (5b)]:

$$CF_3O^- + HNO_3 \rightarrow NO_3^-HF + CF_2O, \quad (5a)$$

$$\rightarrow NO_3^- + CF_3OH. \quad (5b)$$

From the $[NO_3^-]/[NO_3^-HF]$ ratio at small HNO_3 concentrations in the flow tube, the proton transfer channel was found to represent ~7%–8% of the product ion distribution.

The product ions NO_3^- and NO_3^-HF also react with HNO_3 to $NO_3^-HNO_3$ ions. From the decrease of NO_3^-HF as a function of HNO_3 concentration, a lower limit of 1.8×10^{-9} cm^3 $molecule^{-1}$ s^{-1} was derived for the rate constant of the ligand switching reaction of NO_3^-HF with HNO_3.

$$NO_3^-HF + HNO_3 \rightarrow NO_3^-HNO_3 + HF. \quad (6)$$

Apart from bare CF_3O^- ions, small amounts of CF_3O^-HF (105 u) and $CF_3O^-F_2$ (123 u) are also present in the mass spectra without reactant gas addition. At our typical measurement conditions, their concentrations are limited to ~2%–3% of the CF_3O^- concentration. It was found that both ions react with HNO_3 and rate constants of $(2.1 \pm 0.2) \times 10^{-9}$ cm^3 $molecule^{-1}$ s^{-1} and $(4.0 \pm 1.4) \times 10^{-10}$ cm^3 $molecule^{-1}$ s^{-1} were obtained for the reactions of CF_3O^-HF and $CF_3O^-F_2$, respectively. Because of the low abundance of these ions with respect to CF_3O^-, an unambiguous identification of the product ions of these reactions is not obvious. When cooling the walls of the high-pressure ion source with solid CO_2 pellets, $CF_3O^-H_2O$ ions were produced in this section. As described in a previous publication [17], these ions are easily broken up in the low-pressure room temperature part of the flow tube by collisions with the buffer gas. At a typical pressure in the flow tube of 0.53 mbar, the ratio $[CF_3O^-H_2O]/[CF_3O^-]$ at the end of the flow tube is about 1/10, as can be noticed in Fig. 2, where all source and product ions are shown as a function of the HNO_3 concentration in the flow tube.

As thermal decomposition of $CF_3O^-H_2O$ results in formation of CF_3O^- in the reaction zone, the rate constant of CF_3O^- can, in principle, not be inferred from the simple exponential decrease of $[CF_3O^-]$ as a function of $[HNO_3]$ when using the cooled high-pressure ion source. Nevertheless, whether the walls of the high-pressure ion source were at room temperature or at −76°C, the same value was found for the rate constant of reaction (5) as derived using formula (4). This should be the case if CF_3O^- and $CF_3O^-H_2O$ react with HNO_3 with approximately the same rate constant.

The formation of hydrated CF_3O^- is limited to the cooled high-pressure part of the flow tube, as was

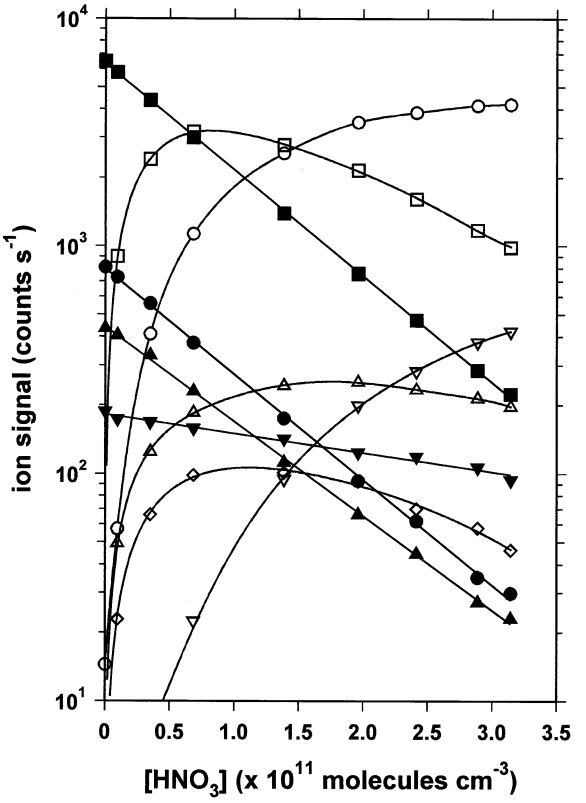

Fig. 2. Evolution of the concentration of the involved ion species as a function of the HNO_3 concentration in the flow tube reactor. Full squares, CF_3O^-; full circles, $CF_3O^-H_2O$; full triangles up, CF_3O^-HF; full triangles down, $CF_3O^-F_2$; open squares, NO_3^-HF; open circles, $NO_3^-HNO_3$; open triangles up, NO_3^-; open diamonds, $CF_3O^-HNO_3$; open triangles down, $NO_3^-(HNO_3)_2$.

checked experimentally by injecting bare CF_3O^- ions, produced in an identical ion source (item 12 in Fig. 1), in the low-pressure part of the flow tube while the high-pressure part was cooled [17].

Therefore, the reaction rate constant of $CF_3O^-H_2O$ with HNO_3 could be determined unambiguously. A value of $(2.1 \pm 0.3)\times10^{-9}$ cm^3 molecule^{-1} s^{-1} was found at 0.53 mbar. Two major product ions were distinguished, apparently formed in the reaction channels (7a) and (7b):

$$CF_3O^-H_2O + HNO_3 \rightarrow CF_3O^-HNO_3 + H_2O, \quad (7a)$$

$$\rightarrow NO_3^-HF + \text{products}. \quad (7b)$$

A simple model calculation of the loss of $CF_3O^-H_2O$ by collisional dissociation and by reaction with HNO_3 and the formation of its reaction products, shows that the relative contribution of the ligand switching channel (7a) to reaction (7) is at most 20%. Evidence that (7b) is the major reaction channel was also obtained by using ambient air as buffer gas at a flow tube pressure of 0.75 mbar. At a relative air humidity of 30%, CF_3O^- and $CF_3O^-H_2O$ were found to be in equilibrium in the reaction zone with a $[CF_3O^-H_2O]/[CF_3O^-]$ ratio of 0.70. Both ions were found to react with nitric acid with rate constants that are in good agreement with those obtained in helium buffer gas with the cooled ion-source configuration. However, since the $CF_3O^-H_2O$ concentration is much higher in the experiments in ambient air and since the decrease of $[CF_3O^-]+[CF_3O^-H_2O]$ at low HNO_3 concentrations is almost compensated by the increase in $[NO_3^-HF]$, it is clear that NO_3^-HF is not only a product ion of CF_3O^- with HNO_3, but that it is also the major product ion of reaction (7).

3.2. Reactions with formic acid

The reaction of bare CF_3O^- with HCOOH was studied at pressures ranging from 0.53 to 1.33 mbar. A pressure-independent rate constant of $(1.7 \pm 0.2) \times 10^{-9}$ cm^3 molecule^{-1} s^{-1} was inferred. Fluoride transfer was discerned to be the main reaction pathway, resulting in $HCOOHF^-$ ions (65 u), which account for at least 94% of the primary product ions observed in the mass spectra.

$$CF_3O^- + HCOOH \rightarrow HCOOHF^- + CF_2O \quad (8)$$

Apart from $HCOOHF^-$ ions, HF_2^- (39 u), $F^-(HF)_2$ (59 u), and CF_3O^-HCOOH (131 u) are also emerging. Their relative contribution to the sum of all primary product ions is ~3.7%, 1.8%, and 1%, respectively. The signal of these ions is clearly correlated with the HCOOH concentration. Nevertheless, it is difficult to conclude whether these ions are products of the reaction of CF_3O^- with HCOOH. This is because of the small amounts of CF_3O^-HF, $CF_3O^-F_2$, and $F^-CF_3OOCF_3$, which are present in the primary ion spectrum as mentioned already in the experimental section. No reaction was observed between the latter two ions and HCOOH, but CF_3O^-HF reacts with HCOOH with a rate constant of $(1.6 \pm 0.2) \times 10^{-9}$ cm^3 molecule^{-1} s^{-1}.

The reaction of $CF_3O^-H_2O$ with HCOOH was found to proceed with a rate constant of $(1.8 \pm 0.2) \times 10^{-9}$ cm^3 molecule^{-1} s^{-1}. Although the ion source conditions were such that CF_3O^-HF was no longer present in the primary ion spectrum, HF_2^-, $F^-(HF)_2$, and CF_3O^-HCOOH still appear as product ions. Their relative contribution to all primary product ions is 4.7%, 6.5%, and 14.7%, respectively. The remaining 74% are $HCOOHF^-$ ions. These are produced by the fluoride transfer reaction of CF_3O^- ions, which result from the break-up of $CF_3O^-H_2O$ ions. From the primary product ion distribution it can be concluded that the main reaction mechanism of $CF_3O^-H_2O$ with HCOOH is ligand switching, leading to CF_3O^-HCOOH product ions, which are present in much higher concentrations than in the case where no $CF_3O^-H_2O$ was produced in the ion source.

The variation of all source and product ions with HCOOH concentration with the cooled ion source configuration is shown in Fig. 3. From this figure it is also clear that the primary product ions $HCOOHF^-$, HF_2^-, $F^-(HF)_2$, and CF_3O^-HCOOH all react with HCOOH. The reaction of $HCOOHF^-$ with HCOOH apparently has two different pathways resulting in the

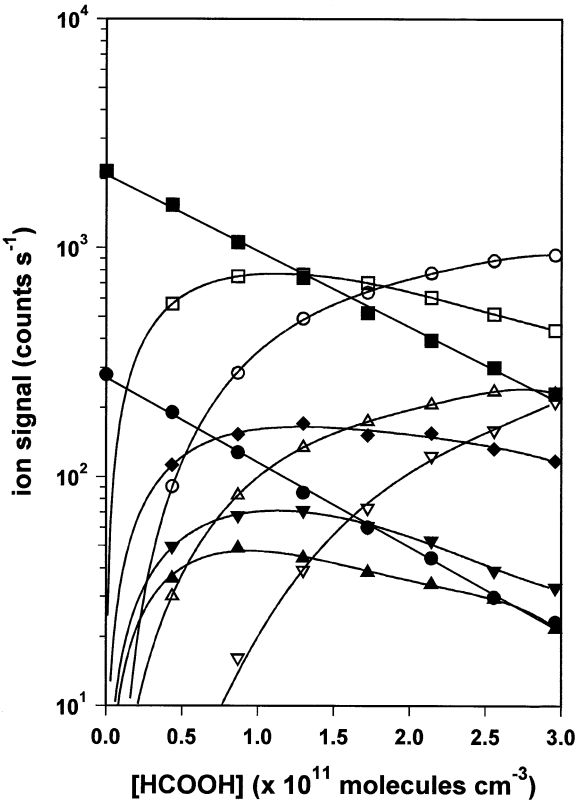

Fig. 3. Evolution of the concentration of the involved ion species as a function of the HCOOH concentration in the flow tube reactor. Full squares, CF_3O^-; full circles, $CF_3O^-H_2O$; open squares, $HCOOHF^-$; open circles, $HCOO^-HCOOH$; open triangles up, $F^-(HCOOH)_2$; open triangles down, $HCOO^-(HCOOH)_2$; full diamonds, CF_3O^-HCOOH; full triangles down, $F^-(HF)_2$; full triangles up, HF_2^-.

biformate anion $HCOO^-HCOOH$ (91 u) and $F^-(HCOOH)_2$ (111 u):

$$HCOOHF^- + HCOOH \rightarrow HCOO^-HCOOH + HF, \quad (9a)$$

$$HCOOHF^- + HCOOH + M \rightarrow F^-(HCOOH)_2 + M. \quad (9b)$$

The latter two ions react further with HCOOH to $HCOO^-(HCOOH)_2$ (137 u):

$$HCOO^-HCOOH + HCOOH + M \rightarrow HCOO^-(HCOOH)_2 + M, \quad (10)$$

$$F^-(HCOOH)_2 + HCOOH \rightarrow HCOO^-(HCOOH)_2 + HF. \quad (11)$$

3.3. Reactions with acetic acid

The reactions with CH_3COOH proceed in a similar way as those with HCOOH. The rate constants of CF_3O^-, CF_3O^-HF, and $CF_3O^-H_2O$ with CH_3COOH were inferred to be, respectively, $(1.5 \pm 0.2) \times 10^{-9}$ cm^3 molecule^{-1} s^{-1}, $(1.0 \pm 0.2) \times 10^{-9}$ cm^3 molecule^{-1} s^{-1} and $(1.6 \pm 0.2) \times 10^{-9}$ cm^3 molecule^{-1} s^{-1}. The major product ion of the reaction of CF_3O^- with CH_3COOH is CH_3COOHF^- (79 u), which is the result of fluoride transfer. This ion accounts for 93% of the primary product ion distribution.

$$CF_3O^- + CH_3COOH \rightarrow CH_3COOHF^- + CF_2O. \quad (12)$$

Next to CH_3COOHF^-, HF_2^- (6%), $F^-(HF)_2$ (<0.5%), and $CF_3O^-CH_3COOH$ (145 u; <0.5%) also appear as primary product ions. Again, it is difficult to assess whether these effectively are reaction products of CF_3O^- with CH_3COOH or whether they are reaction products of CF_3O^-HF with CH_3COOH. As in the case of HCOOH, no reaction was observed for $CF_3O^-F_2$ or $F^-CF_3OOCF_3$ with CH_3COOH.

When cooling the high-pressure ion source, the product ion distribution changes as follows: CH_3COOHF^- (80%), HF_2^- (8%), $F^-(HF)_2$ (<0.5%), and $CF_3O^-CH_3COOH$ (12%). This leads to the conclusion that ligand switching is the major reaction mechanism of $CF_3O^-H_2O + CH_3COOH$.

$$CF_3O^-H_2O + CH_3COOH \rightarrow CF_3O^-CH_3COOH + H_2O. \quad (13)$$

Again, the primary reaction products are subject to secondary reactions. The CH_3COOHF^- ion reacts with CH_3COOH via two pathways to produce either the biacetate anion $CH_3COO^-CH_3COOH$ (119 u) or $F^-(CH_3COOH)_2$ (139 u). The latter two react with

CH_3COOH to form $CH_3COO^-(CH_3COOH)_2$ (179 u) ions.

$$CH_3COOHF^- + CH_3COOH \rightarrow CH_3COO^-CH_3COOH + HF, \quad (14)$$

$$CH_3COOHF^- + CH_3COOH + M \rightarrow F^-(CH_3COOH)_2 + M, \quad (15)$$

$$CH_3COO^-CH_3COOH + CH_3COOH + M \rightarrow CH_3COO^-(CH_3COOH)_2 + M, \quad (16)$$

$$F^-(CH_3COOH)_2 + CH_3COOH \rightarrow CH_3COO^-(CH_3COOH)_2 + HF. \quad (17)$$

The evolution of all ion species involved in the reactions with CH_3COOH when using the cooled high-pressure ion source is shown in Fig. 4.

The overall uncertainty on the rate constants of the ion/molecule reactions with HNO_3 and with the carboxylic acids is estimated to be 25% and 30%, respectively.

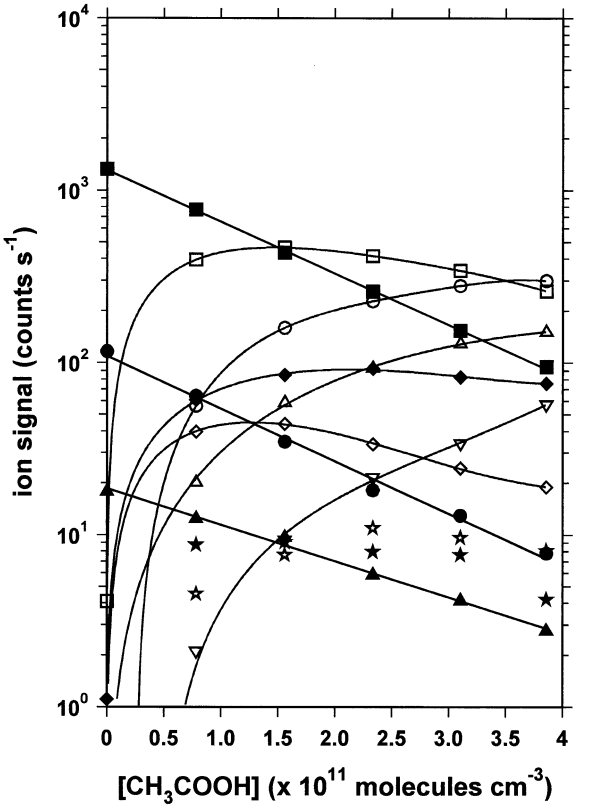

Fig. 4. Evolution of the concentration of the involved ion species as a function of the CH_3COOH concentration in the flow tube reactor. Full squares, CF_3O^-; full circles, $CF_3O^-H_2O$; full triangles up, CF_3O^-HF; open squares, CH_3COOHF^-; open circles, $CH_3COO^-CH_3COOH$; open triangles up, $F^-(CH_3COOH)_2$; open triangles down, $CH_3COO^-(CH_3COOH)_2$; full diamonds, $CF_3O^-CH_3COOH$; open diamonds, HF_2^-; open stars, $HF_2^-CH_3COOH$; full stars, mass 63 (unidentified).

4. Discussion

4.1. Reactions with HNO_3

The rate constant of bare CF_3O^- with HNO_3 in the pressure range 0.53–1.33 mbars (2.3×10^{-9} cm^3 molecule^{-1} s^{-1}) is in very good agreement with the value reported by Huey et al. [15] (2.2×10^{-9} cm^3 molecule^{-1} s^{-1}) at ~0.53 mbar. Taking into account a measured value of 2.17 D for the dipole moment of HNO_3 [46] and an estimated value of (3–10) $\times 10^{-30}$ m^3 for its polarizability [15], a value of (1.7–2.1) $\times 10^{-9}$ cm^3 molecule^{-1} s^{-1} is obtained for the collisional rate constants of CF_3O^-, $CF_3O^-H_2O$, and CF_3O^-HF with HNO_3 using the parameterized formula of Su and Chesnavich [47] based on trajectory calculations. Comparison with our experimental values shows that the reactions are taking place indeed at the gas kinetic rate.

As reported in the "Results" section, the major reaction product of $CF_3O^-H_2O$ with HNO_3 appears to be NO_3^-HF. This is in agreement with the in situ mass spectra obtained with our balloon-borne CIMS apparatus in the stratosphere when using a CF_3O^- ion source [48]. As explained in the "Introduction" section, the appearance of $CF_3O^-HNO_3$ in the flight spectra led to the assumption that $CF_3O^-H_2O$ ions react with HNO_3 by ligand switching. However, at conditions where CF_3O^- and $CF_3O^-H_2O$ are expected to be in equilibrium in the reaction zone of the flow tube of the balloon-borne instrument, the ratio $([NO_3^-HF]+[NO_3^-])/[CF_3O^-HNO_3]$ is also 10 to 30 times higher than the ratio $[CF_3O^-]/[CF_3O^-H_2O]$.

4.2. Reactions with the carboxylic acids

As the fluoride affinities of HCOOH and CH_3COOH are higher than that of CF_2O [49], reactions (8) and (12) are exothermic, and therefore, fluoride transfer from CF_3O^- to HCOOH and CH_3COOH is very likely to take place. Although the reaction of CF_3O^- with HCOOH has already been studied by Huey et al. [50] in a search for proton transfer channels to determine the gas phase acidity of CF_3OH by a bracketing mechanism, no rate constant for the fluoride transfer reaction of CF_3O^- has been reported. The fluoride transfer reaction of CF_3O^- with CH_3COOH has also been studied in the literature [51], but no rate constants were reported either. Using a value of 1.41 D for the dipole moment of HCOOH and a value of 3.4×10^{-30} m^3 for its polarizability [46], a value of $(1.4–1.5) \times 10^{-9}$ cm^3 $molecule^{-1}$ s^{-1} is calculated for the collisional rate constants of CF_3O^-, $CF_3O^-H_2O$, and CF_3O^-HF with HCOOH. The experimentally obtained values are at most 20% larger than the gas kinetic rate constant. As this is well within the error bars, we can conclude that these reactions also proceed at the collision rate.

The collision rate constants of CF_3O^-, $CF_3O^-H_2O$, and CF_3O^-HF with CH_3COOH were calculated to be $(1.6–1.7) \times 10^{-9}$ cm^3 $molecule^{-1}$ s^{-1} by taking a value of 1.70 D for the dipole moment of CH_3COOH and 5.1×10^{-30} m^3 for its polarizability [46]. The experimental rate constants for the reactions of CF_3O^- and $CF_3O^-H_2O$ with CH_3COOH are in this case some 10% lower than the collision limit, which is again well within experimental error.

Contrary to the reactions with HNO_3, ligand switching seems to be a more important mechanism for the reactions of $CF_3O^-H_2O$ and CF_3O^-HF with HCOOH and CH_3COOH. Other possible product ions are HF_2^-, $F^-(HF)_2$, $HCOOHF^-$, or CH_3COOHF^-. The simultaneous presence of different source ions in the flow tube, however, makes it impossible to quantify the individual contributions of all product ions to the product ion distributions of the reactions of $CF_3O^-H_2O$ and CF_3O^-HF with HCOOH and CH_3COOH.

Although it is not possible to determine unambiguously whether or not the reaction of CF_3O^- with HCOOH is a possible production mechanism of HF_2^- ions, it is found that the exothermicity of reaction (18) is ranging from -45.9 kJ mol^{-1} to -120.4 kJ mol^{-1}, depending on which value is used for the heat of formation of CF_3O^- [49,52].

$$CF_3O^- + HCOOH \rightarrow HF_2^- + CO_2 + CFOH. \quad (18)$$

As the fluorine affinities of HCOOH and CH_3COOH are higher than that of HF [49], the primary product ion HF_2^- will probably react with HCOOH and CH_3COOH by fluoride transfer. Apart from the mentioned considerations, thermochemical data for most of the ionic species involved in this study are nonexisting, and therefore, it is hard to speculate about the occurrence of possible reaction channels in most cases.

4.3. Implications for the measurement of HNO_3, HCOOH and CH_3COOH concentrations by CIMS

An important result of our laboratory measurements is that CF_3O^-, $CF_3O^-H_2O$, and CF_3O^-HF react with nitric acid with rate constants that do not differ from each other by more than 10%. This justifies our previously used approach [16,48], where the HNO_3 concentration is calculated using the simple formula

$$[HNO_3] = \frac{1}{k_{av}\tau} \times \ln\left(1 + \frac{[P^-]}{[S^-]}\right), \quad (19)$$

where $[S^-]$ is the sum of the source ion concentrations ($[CF_3O^-] + [CF_3O^-H_2O] + [CF_3O^-HF]$) and $[P^-]$ is the sum of the primary product ion concentrations ($[NO_3^-HF] + [NO_3^-] + [CF_3O^-HNO_3]$) and of the secondary product ions (e.g., $NO_3^-HNO_3$) formed by further reaction of the primary product ions. For k_{av} a weighted average of the rate constants of CF_3O^-, $CF_3O^-H_2O$ and CF_3O^-HF with HNO_3 is taken and τ is the reaction time, which is measured regularly in situ. Application of this formula to the flight data resulted in HNO_3 mixing ratio height profiles which are in reasonable agreement with data obtained by other groups using other experimental techniques [48]

and with data obtained by the same technique using other reaction schemes [16].

For the time being, the use of a CF_3O^- ion source for HCOOH and CH_3COOH detection by CIMS is less straightforward. Although ligand switching most likely is the major reaction mechanism of the reactions of $CF_3O^-H_2O$ with HCOOH and CH_3COOH, the contribution of HF_2^- and $F^-(HF)_2$ cannot be neglected. The latter two ions, which can also be the product ions of the reactions with CF_3O^-HF, bear no fingerprints of HCOOH and CH_3COOH. They cannot be considered as selective product ions and are, therefore, not suitable for the CIMS-detection of these carboxylic acids. In atmospheric applications this problem might perhaps be circumvented by performing measurements in dry regions (e.g., near the tropopause onboard an aircraft) using a heated flow tube to decrease the contribution of $CF_3O^-H_2O$ and CF_3O^-HF to the primary ion spectrum.

Nevertheless, the laboratory measurements of bare CF_3O^- with HCOOH and CH_3COOH show that these reactions are very selective and lead to an almost unique reaction product. As a consequence, CF_3O^- would certainly be useful as a chemical ionization precursor ion for the detection of HCOOH and CH_3COOH in laboratory kinetic studies where these neutrals are involved.

References

[1] G. Knop, F. Arnold, Planet. Space Sci. 33 (1985) 983.
[2] A.A. Viggiano, Mass Spectrom. Rev. 12 (1993) 115.
[3] S. Spreng, F. Arnold, Geophys. Res. Lett. 21 (1994) 1251.
[4] F. Arnold, S. Spreng, Geophys. Res. Lett. 21 (1994) 1255.
[5] F. Arnold, T. Stilp, R. Busen, U. Schumann, Atmos. Environ. 32 (1998) 3073.
[6] D.J. Tanner, A. Jefferson, F.L. Eisele, J. Geophys. Res. 102 (1997) 6415.
[7] F.L. Eisele, D.J. Tanner, J. Geophys. Res. 98 (1993) 9001.
[8] J. Schneider, V. Bürger, F. Arnold, J. Geophys. Res. 102 (1997) 25501.
[9] R.L. Mauldin III, D.J. Tanner, F.L. Eisele, J. Geophys. Res. 103 (1998) 3361.
[10] T. Reiner, M. Hanke, F. Arnold, H. Ziereis, H. Schlager, W. Junkermann, J. Geophys. Res. 104 (1999) 18647.
[11] L.G. Huey, E.J. Dunlea, E.R. Lovejoy, D.R. Hanson, R.B. Norton, F.C. Fehsenfeld, C.J. Howard, J. Geophys. Res. 103 (1998) 3355.
[12] F. Arnold, V. Bürger, K. Gollinger, M. Roncossek, J. Schneider, S. Spreng, J. Atmos. Chem. 30 (1998) 49.
[13] U. Schumann, H. Schlager, F. Arnold, J. Ovarlez, H. Kelder, O. Hov, G. Hayman, I.S.A. Isaksen, J. Staehelin, P.D. Whitefield, J. Geophys. Res. 105 (2000) 3605.
[14] T.M. Miller, J.O. Ballenthin, R.F. Meads, D.E. Hunton, W.F. Thorn, A.A. Viggiano, Y. Kondo, M. Koike, Y. Zhao., J. Geophys. Res. 105 (2000) 3701.
[15] L.G. Huey, P.W. Villalta, E.J. Dunlea, D.R. Hanson, C.J. Howard, J. Phys. Chem. 100 (1996) 190.
[16] E. Arijs, A. Barassin, E. Kopp, C. Amelynck, V. Catoire, H.P. Fink, C. Guimbaud, U. Jenzer, D. Labonnette, W. Luithardt, E. Neefs, D. Nevejans, N. Schoon, A.M. Van Bavel, Int. J. Mass Spectrom. 181 (1998) 99.
[17] C. Amelynck, A.M. Van Bavel, N. Schoon, E. Arijs, Int. J. Mass Spectrom., 202 (2000) 207.
[18] World Meteorological Organization, Global Ozone Research and Monitoring Project, Report 16, Atmospheric Ozone 1985, Assessment of our understanding of the processes controlling its present distribution and change, and references therein, Vol. 2, 1985.
[19] World Meteorological Organization, Global Ozone Research and Monitoring Project, Report 37, Scientific Assessment of Ozone Depletion: 1994, and references therein, 1994.
[20] J.N. Galloway, G.E. Likens, Atmos. Environ. 15 (1981) 1081.
[21] M.M. Abbas, V.G. Kunde, J.C. Brasunas, J.R. Herman, S.T. Masie, J. Geophys. Res. 96 (1991) 10885.
[22] J.C. Gille, P.L. Bailey, C.A. Graig, Adv. Space Res. 18 (1996) 125.
[23] J.B. Kumer, J.L. Mergenthaler, A.E. Roche, R.W. Nightingale, G.A. Ely, W.G. Uplinger, J.C. Gille, S.T. Massie, P.L. Bailey, M.R. Gunson, M.C. Abrams, G.C. Toon, B. Sen, J.-F. Blavier, R.A. Stachnik, C.R. Webster, R.D. May, D.G. Murcray, F.J. Murcray, A. Goldman, W.A. Traub, K.W. Jucks, D.G. Johnson, J. Geophys. Res. 101 (1996) 9621.
[24] M. Koike, Y. Kondo, H. Irie, F.J. Murcray, J. Williams, P. Fogal, R. Blatherwick, C. Camy-Peyret, S. Payan, H. Oelhaf, G. Wetzel, W. Traub, D. Johnson, K. Jucks, G.C. Toon, B. Sen, J.F. Blavier, H. Schlager, H. Ziereis, N. Toriyama, M.Y. Danilin, J.M. Rodriguez, J. Kanzawa, Y. Sasano, J. Geophys. Res. 105 (2000) 6761.
[25] A.L. Lazrus, B.W. Ganrud, J. Atmos. Sci. 31 (1974) 1102.
[26] A. Chebbi, P. Carlier, Atmos. Environ. 30 (1996) 4233.
[27] J. Galloway, G.E. Likens, W.C. Keene, J.M. Miller, J. Geophys. Res. 87 (1982) 8771.
[28] W.C. Keene, R.W. Talbot, M.O. Andreae, K. Beecher, H. Berresheim, M. Castro, J.C. Farmer, J.N. Galloway, M.R. Hoffmann, S.M. Li, J.R. Maben, J.W. Munger, R.B. Norton, A.A.P. Psenny, H. Puxbaum, H. Westberg, W. Winiwarter, J. Geophys. Res. 94 (1989) 6457.
[29] P.L. Hanst, N.W. Wong, J. Bragin, Atmos. Environ. 16 (1982) 969.
[30] A. Goldman, F.H. Murcray, D.G. Murcray, C.P. Rinsland, Geophys. Res. Lett. 4 (1984) 307.
[31] C. Rinsland, A. Goldman, Appl. Opt. 31 (1992) 6969.
[32] R.J. Yokelson, D.W.T. Griffith, J. Geophys. Res. 101 (1996) 21067.

[33] R.J. Yokelson, R. Susott, D.E. Ward, J. Reardon, D.W.T. Griffith, J. Geophys. Res. 102 (1997) 18865.
[34] A. Perrin, C.P. Rinsland, A. Goldman, J. Geophys. Res. 104 (1999) 18661.
[35] E.G. Chapman, D.V. Kenny, K.M. Busness, J.M. Thorp, C.W. Spicer, Geophys. Res. Lett. 22 (1995) 405.
[36] L.G. Huey, E.R. Lovejoy, Int. J. Mass Spectrom. Ion Processes 155 (1996) 133.
[37] T. Reiner, O. Möhler, F. Arnold, J. Geophys. Res. 104 (1999) 13943.
[38] J. Viidanoja, T. Reiner, F. Arnold, Int. J. Mass Spectrom. 181 (1998) 31.
[39] S.R.M. Ellis, J.R. Thwaites, J. Appl. Chem. 7 (1957) 157.
[40] C. Amelynck, D. Fussen, E. Arijs, Int. J. Mass Spect. Ion Processes 133 (1994) 13.
[41] J. Burkholder, R.K. Talukdar, A.R. Ravishankara, S. Solomon, J. Geophys. Res. 98 (1993) 22937.
[42] L.G. Huey, D.R. Hanson, C.J. Howard, J. Phys. Chem. 99 (1995) 5001.
[43] R. Büttner and G. Maurer, Ber. Bunsen-Ges. Phys. Chem. 87 (1983) 877.
[44] P.H. Wine, R.J. Astalos, R. Mauldin III, J. Phys. Chem. 89 (1985) 2620.
[45] M. Finkbeiner, P. Neeb, O. Horie, G.K. Moortgat, Fresenius' J. Anal. Chem. 351 (1995) 521.
[46] D.R. Lide (Ed.), CRC Handbook of Chemistry and Physics, CRC, Boca Raton, 1999.
[47] T. Su, W.J. Chesnavich, J. Chem. Phys. 76 (1982) 5183.
[48] N. Schoon, C. Stépien, C. Amelynck, E. Arijs, E. Neefs, D. Nevejans, V. Catoire, D. Labonnette, G. Poulet, H.-P. Fink, E. Kopp, W. Luithardt, in: European Communities (Ed.), Air pollution research report on stratospheric ozone, Proceedings of the Fifth European Workshop, 27 September–1 October 1999, St.-Jean de Luz (France).
[49] J.W. Larson, T.B. McMahon, J. Am. Chem. Soc. 105 (1983) 2944.
[50] L.G. Huey, E.J. Dunlea, C.J. Howard, J. Phys. Chem. 100 (1996) 6504.
[51] T.B. McMahon, C.J. Northcott, Can. J. Chem. 56 (1978) 1069.
[52] R.W. Taft, I.J. Koppel, R.D. Topsom, F. Anvia, J. Am. Chem. Soc. 112 (1990) 2047. AQ—1 AUTHOR: Sentence ("It turned out,...") ok with changes made?